Journal of Solid State Chemistry 201 (2013) 153–163

Contents lists available at SciVerse ScienceDirect

Journal of Solid State Chemistry

journal homepage: www.elsevier.com/locate/jssc

Synthesis of crumpled nanosheets of polymeric carbon nitride from melamine cyanurate

Roberto C. Dante [a,*], Pablo Martín-Ramos [a], F.M. Sánchez-Arévalo [b], L. Huerta [b], M. Bizarro [b], Luis M. Navas-Gracia [a], Jesús Martín-Gil [a]

[a] Laboratorio de Materiales Avanzados (Advanced Materials Laboratory) ETSIIAA, Universidad de Valladolid, Avenida de Madrid 44, 34004 Palencia, Spain
[b] Instituto de Investigaciones en Materiales, Universidad Nacional Autónoma de México, Apdo. Postal 70-360, Cd. Universitaria, Mexico, D.F. 04510, Mexico

ARTICLE INFO

Article history:
Received 10 December 2012
Received in revised form
5 February 2013
Accepted 11 February 2013
Available online 7 March 2013

Keywords:
Polymeric carbon nitride
Graphene
Melamine cyanurate
Heptazine

ABSTRACT

Polymeric carbon nitride was synthesized by pyrolysis in nitrogen flux at different temperatures between 450 and 700 °C using melamine cyanurate as a reagent and sulfuric acid as a catalyst. The obtained carbon nitride consisted of curled nanosheets (650 °C), and globular particles (700 °C) with formula $C_6N_7NHNH_2$. The reaction yield of the catalyzed reaction was around the 15% for the sample treated at 700 °C, in a tapped crucible. The optical band gap of the polymer obtained at 700 °C is around 2.9 eV. The gap to the Fermi level is around 2 eV, considerably above the half of the band gap (due to electrons trapped in the gap), indicating that the polymer is probably a *n*-type semiconductor.

1. Introduction

The great interest around carbon nitride began in 1990, when the theoretical study by Cohen [1] and Liu and Cohen [2] predicted that α-, β-, and cubic-C_3N_4 ($CN_{x=1.33}$) should have a bulk modulus comparable or higher than the bulk modulus of diamond. Melamine polymers have the right ratio of nitrogen to carbon to be the precursor of carbon nitride $CN_{x=1.33}$. Nevertheless, the attempts to pyrolyze melamine have led to a great variety of sp^2 hybridized materials [3–5]. Graphitic carbon nitride is regarded as the most promising candidate to complement carbon materials in various potential applications. Apart from its applications as the precursor for the synthesis of superhard carbon nitride phases, it has also been investigated for a number of other applications including: mesoporous materials [6], high performance tribological coatings, nitrogen source for the synthesis of metal nitrides [7], precursor for the preparation of carbon nitride nano/microstructures [8,9], as a metal-free catalyst for several "biomimetic" reactions, including CO_2 fixing and activation, and some Friedel–Crafts reactions, as reported by Thomas et al. [10].

Li et al. [11] reported the synthesis of nitrogen-rich graphitic carbon nitrides via a route based on the polycondensation reaction between melamine and cyanuric chloride in the presence of nickel powder. This route leads to *g*-CN_x, with high nitrogen ratio $x=1.6$, opening the pathway towards the synthesis of large amounts of graphitic carbon nitrides to be studied for different applications. For example, carbon nitride graphene form a new family of wide-gap semiconducting materials, in which the gap can be tuned by small variations in stress applied to the layers or by the presence of adatoms [12]. For this reason, it is interesting to develop a method to obtain monolayers (graphene) of carbon nitride.

The pathway presented by Li et al. was extended to heteroatoms different from halogens by Dante et al. [13]. Prior to this work, Dante et al. carried out a solid state polycondensation using uric acid, as the precursor of cyanuric acid, and melamine.

In the research described here, the polycondensation reaction (see Eq. (1)) was carried out starting directly from melamine cyanurate—the adduct of melamine and cyanuric acid which crystallizes in layers like graphite [13].

$$C_3N_3(NH_2)_3 \bullet C_3N_3(OH)_3 \rightarrow C_6N_7(NH)(NH_2) + 3H_2O \quad (I)$$

This reaction, as shown hereafter, is promoted by sulfuric acid, which, we suggest, may act as a catalyst. This hypothesis was based on the work of Heine et al., who reported the formation of melaminium sulfate [14] more stable than melamine cyanurate, which sublimates around 430 °C. In our report, the results of the melamine cyanurate pyrolized in the range between 450 and 700 °C are reported, with the significant result being the formation of crumpled and globular particles of polymeric carbon nitride with thickness in the 10–25 nm range.

* Corresponding author.
E-mail address: rcdante@yahoo.com (R.C. Dante).

0022-4596/$ - see front matter © 2013 Elsevier Inc. All rights reserved.
http://dx.doi.org/10.1016/j.jssc.2013.02.016

The product obtained at 700 °C showed peaks in X-ray photoelectron spectroscopy (XPS) which corresponded to a polymer based on heptazine units. This result was also confirmed by means of Fourier transform infrared spectroscopy. Low binding energy XPS spectra complemented the information about the band gap, obtained by ultraviolet–visible (UV–vis) spectroscopy, revealing the *n*-type semiconducting characteristics of the material [15]. Transmission electron microscopy (TEM) showed flakes with wrapped or crumpled edges, filamentous and tubular particles with nano-sized sections up to 650 °C, and finally globular particles at 700 °C. Moreover, X-ray powder diffraction (XRPD) showed a marked sharpening, intensification and shift of the peak to a tighter interplanar distance, which corresponds to the tightening of the graphene stacks by temperature increment, especially for the product obtained at 700 °C.[1]

2. Materials and experimental methods

The reagent, melamine cyanurate, was supplied by Ferro-plast S.r.l. (Italy) with a purity higher than 99%. Melamine cyanurate was manually milled in an agate mortar for about 5 min; subsequently 30 g of sample were treated overnight (12 h) with 25 mL of 1 M sulfuric acid in a beaker at room temperature, with no stirring and without any dissolution, and subsequently dried in air at 110 °C for 6 h. In order to have a reference, the same thermal treatments and experiments were conducted on the reagent alone (reference) and on the sulfuric acid-treated sample (SATS). The samples, of about 4 g, were placed in a tapped ceramic crucible and thermally treated at 650 °C for 50 min in a convective tubular oven GVA 12/900, power: 5.460 kW, heating length: 900 mm, T_{max}: 1200 °C (Carbolite, UK) under nitrogen flux.

A thermal gravimetric analysis instrument (TGA), equipped with differential thermal analysis (DTA) TGA/SDTA851e/SF/1100 (Mettler-Toledo, USA), was used to heat the samples at a rate of 1 °C min^{-1} in nitrogen flux to determine their thermal behavior and identify the eventual reaction steps. The infrared spectra were obtained by means of a Thermo Nicolet 380 Fourier transform-infrared (FT-IR) spectrophotometer (Nicolet, USA) with tablets of the specimens mixed with KBr (1 mg of sample in 100 mg of KBr) in order to identify the chemical functional groups.

The X-ray diffraction patterns were obtained by means of a powder diffractometer ENRAF-NONIUS FR590, detector INEL CPS 120 (BRUKER AXS, The Netherlands), with monochromator-quartz discriminator, Debey–Scherrer geometry, using Cu *K*α radiation, and glass capillaries for sample mounting. Transmission electron microscopy (TEM) was performed with a JEOL JEM-FS2200 HRP (JEOL, Japan) and scanning electron microscopy by a JEOL JSM-820 SEM with energy-dispersive X-ray spectroscopy (EDS) probe (JEOL, Japan). The content of carbon, nitrogen and hydrogen was determined by means of a Carlo Erba analyzer CHNS-O EA 1108 (Carlo Erba, Italy). This analysis method is based on the complete and instantaneous oxidation of the sample by "flash combustion".

XPS measurements were executed to determine the chemical bond interactions. The instrument used was an UHV system of VG Microtech ESCA2000 Multilab. This equipment has an Al *K*α X-ray source (1486.60 eV), and a CLAM4 MCD analyzer. The XPS spectra were fitted with the program SDP v 4.1.

The diffuse reflectance spectra of the samples were obtained by means of a UV–visible Spectrophotometer Perkin Elmer Lambda 35 equipped with an integration sphere. Spectralon was used as a reference. An analysis of the reflectance spectra was carried out to obtain the band gap following the method of the Kubelka–Munk function $F(R)$. The band gap value was calculated through the intersection of the straight-line extrapolation below and above the high photon energy knee of the $F(R)$ curve [16].

3. Results and discussion

3.1. Thermal behavior and reaction yield

The TGA curve of the reference, reported in Fig. 1, shows a huge loss starting from 380 °C with a sharp endothermic DTA peak at 443 °C, which corresponds to sublimation. Above 450 °C, the residue polymerizes, and finally decomposes with a small exothermic peak at 699 °C. It is noteworthy to point out that there is a broad endothermic peak from 520 °C to 690 °C with an apparent small peak at 620 °C. This is presumably due to the variation of the specific heat while the material was transforming before the final decomposition. On the other hand, the TGA of the SATS (Fig. 1) showed several gradual losses between 280 °C and 480 °C, which correspond mainly to the dehydration, ammonia and sulfuric acid release caused by polycondensation. In this case the exothermic peak around 700 °C is present, as in the reference, and may be associated to a specific arrangement of the polymer, such as stacking and crystallization, but in this case it appears only as a shoulder of a much stronger exothermic DTA peak at 738 °C (Fig. 1) which can be attributed to the final decomposition of the product (that in the reference case was not observed due to the very low reaction yield). It should also be pointed out that the same broad endothermic peak, observed in the reference, is presumably covered by the overlapping of the strong exothermic peak in SATS. These TGA experiments show that sulfuric acid promoted the polymerization before sublimation, and that the reaction yield was about the 25% at 600 °C and the 11% by weight at 700 °C, while for the reference the reaction yield was less than 5% at 600 °C and almost null at 700 °C in the analysis conditions due to the free flow of gases including reactive polymeric fragments. As shown by Yan et al. [17], higher sulfuric acid concentrations did not lead to different products or yields, while very low ones are ineffective. It is noteworthy to point out that the yields with tapped crucibles were higher than those found by TGA in all cases, due to the retention of the decomposition polymeric fragments. They were approximately 15%, and the 5% at 700 °C for SATS and the reference, respectively.

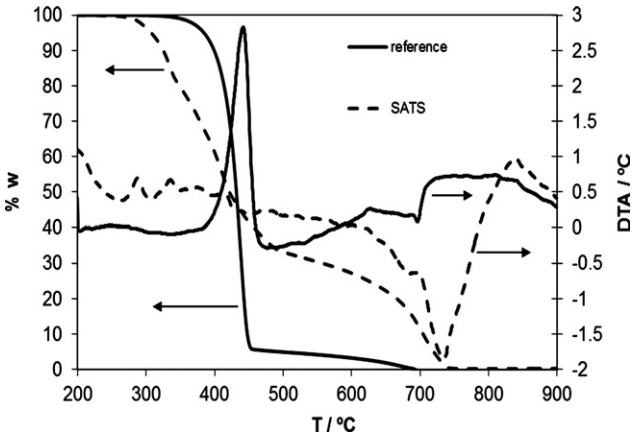

Fig. 1. TGA and DTA of melamine cyanurate as-is and the sulfuric acid-treated sample (SATS) of melamine cyanurate.

[1] Two TEM images of these polymeric carbon nanosheets were shown in the Materials Today Virtual Conference *Frontiers of Microscopy* held on March 21st 2012.

3.2. Physical–chemical characterization

3.2.1. Fourier transform infrared spectroscopy

Sulfuric acid modified the IR spectrum of melamine cyanurate in a dramatic manner. The corresponding IR spectrum taken before the thermal treatments was reported and discussed in detail in a previous short communication [18]. In summary, the main effects of sulfuric acid were the shifting of the cyanuric acid from the lactam tautomer to the lactim one, and the formation of strong hydrogen bonds between the amino groups of melamine and the oxygen of sulfate forming a relatively stable adduct $[(LH_2)_2(SO_4)_2]_n$ (L=melamine, n=number of monomers) described in detail by Heine et al. [14] and also detected by us through single crystal XRD but not reported for brevity.

The FT-IR spectra of the reference treated at different temperatures between 450 °C and 700 °C are shown in Fig. 2 (full spectra) and 3 (between 2000 and 500 cm^{-1}), and respectively those of treated SATS are shown in Figs. 4 and 5. The bands between 3500 and 3000 cm^{-1} are due to NH stretching (Figs. 2 and 4) and evolve towards a definition of four bands from 450 °C to 700 °C, where the bands at 3248, 3150 and 3078 cm^{-1} are due to NH interacting via hydrogen bond (Fig. 2). The band at 1637 cm^{-1} is assigned to the conjugated CN stretching, and the other bands between 1574 and 1459 cm^{-1} belong to stretching modes of the tri-*s*-triazine ring. The peak at 1406 cm^{-1} may belong to the C–N stretching of the tertiary bridging nitrogen in the mid of the tri-*s*-triazine ring, the others between 1315 and 1204 cm^{-1} to secondary bridging nitrogen (all associated with the four bands of NH stretching) [19], and primary amines. The peak at 892 cm^{-1} can be associated with a mode of cross-linked heptazine deformation. The sharp peak at 813 cm^{-1} can be assigned to a tri-*s*-triazine ring mode of bending [13,20]. The bands between 1574 and 1540 cm^{-1}, as well as that at 1459 cm^{-1}, related to heptazine units formation, grew from 450 °C to 700 °C. The bands at 1238 and 1204 cm^{-1}, related to secondary

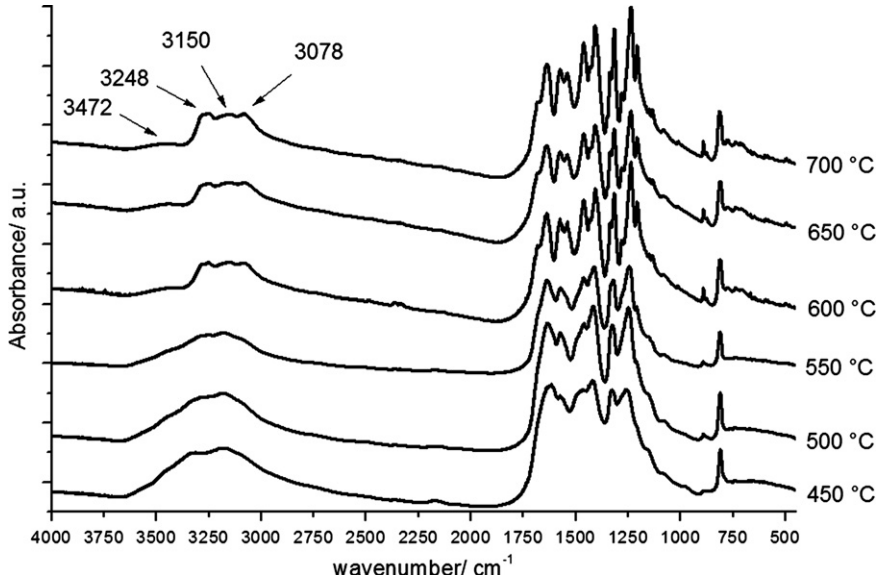

Fig. 2. Full FT-IR spectra of melamine cyanurate as-is.

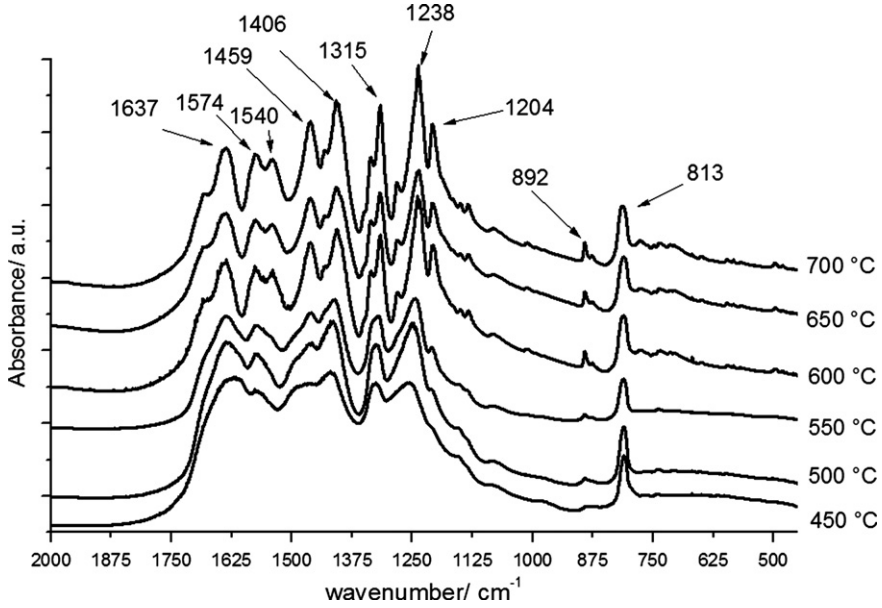

Fig. 3. FT-IR spectra of melamine cyanurate as-is in the 2000–450 cm^{-1} range.

bridging amines also increased due to cross-linking between heptazine units from 450 °C to 700 °C, and that at 892 cm^{-1} grew from 450 °C to 700 °C, with a simultaneous increase in the secondary amine bands, which correspond to cross-linked heptazine bending (Figs. 2 and 3). In both cases, reference's and SATS's band grew with the increasing temperature due to polymer growth. Peaks' sharpening and definition (Figs. 2–5) with the temperature increase are also exhibited, possibly due to stacking arrangement as inferred by XRPD measurements. It is worth mentioning the presence of a low band at 2165 cm^{-1} attributable to the stretching of cyano groups –C≡N as indicated in Fig. 4, probably representative of a step in the ring formation [13]. The FT-IR spectra of reference and SATS at 650 °C and 700 °C correspond substantially to a melon (polymeric carbon nitride) (Fig. 5), which is known to consist of heptazine units (see reference [21] for more details). Identical FT-IR spectra were obtained for the reference treated at 650–700 °C (Fig. 3), confirming that the products were the same and that sulfuric acid acted mainly as catalyst.

3.2.2. Elemental analysis

Based on the elemental analysis, the ratio of nitrogen to carbon changed from 1.67 at 450 °C to 1.45 at 700 °C for both SATS and the reference, approaching the theoretical value of 1.33 of full carbon nitride. In Table 1 the elemental analysis data are reported for both reference and SATS and for all the treatment temperature levels. No sulfur was appreciably detected. For SATS at 700 °C, the weight percentages of C, N and H were: 60.93%, 36.10%, and 1.49 %, while for the reference they were 60.54%, 35.85%, and 1.50%. The found empirical formula was $C_6N_9H_3$ (i.e. $C_6N_7NHNH_2$) for both SATS and the reference treated at 700 °C, which corresponds to the melon empirical formula, i.e. polymeric carbon nitride, in full accordance with the IR results.

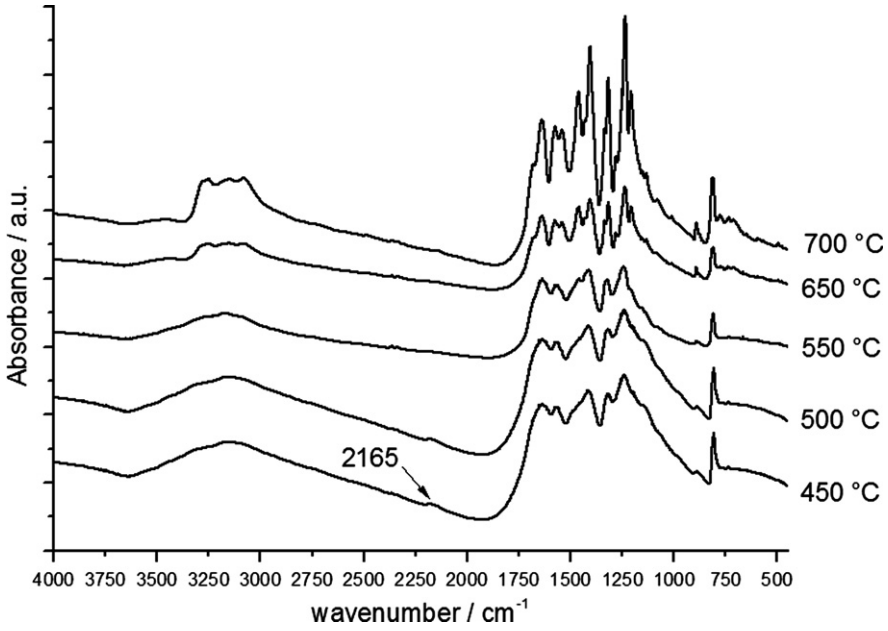

Fig. 4. Full FT-IR spectra of the sulfuric acid-treated sample (SATS) of melamine cyanurate.

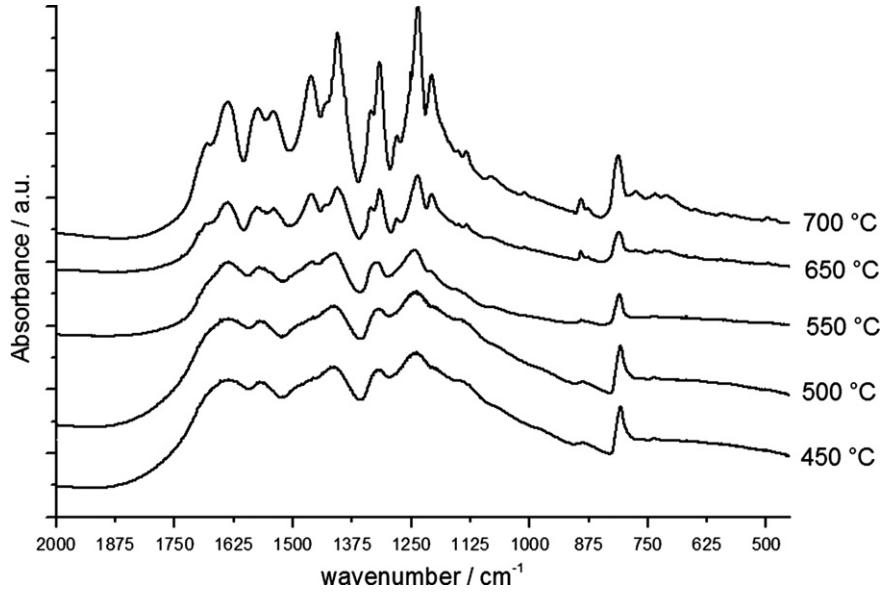

Fig. 5. FT-IR spectra of the sulfuric acid-treated sample (SATS) of melamine cyanurate in the 2000–450 cm^{-1} range.

3.2.3. X-ray photoelectron spectroscopy

Fig. 6 shows the evolution of the XPS spectra as a function of the treatment temperature for both the reference and SATS. A detailed analysis of the C1s and N1s spectra has been carried out. At a first glance, it is possible to notice that the O1s peak, around 532 eV, decreased in intensity from 450 °C to 700 °C for both the reference and SATS. In the case of SATS the values of binding energy changed from a maximum at around 531 eV, characteristic of inorganic oxygen, at 450 °C to 532 eV, characteristic of organic oxygen, at 700 °C. However, SATS at 450 °C exhibits a higher peak than that of the reference at the same temperature due to the treatment with sulfuric acid. At 700 °C the O1s peak of both samples are quite similar and very low. Moreover, SATS at 450 °C exhibits also S2s and S2p peaks, although very weak, due to the treatment with sulfuric acid. At higher temperatures S was not detected any more. The basic unit of the polymer is shown in Fig. 7 for one of the resonance structures, in order to favor the identification of the atom types. Each atom is numbered and the assignment carried out by XPS follows this labeling system. The C1s and N1s spectrum for the temperature range 450–700 °C and their corresponding deconvolution curves are shown in Fig. 8 for the reference. For the sample treated at 450 °C, it is possible to notice that there are carbon atoms of intermediates with C═N, C–C and C–N bonds; however, the carbons named C_1 and C_2 (see Fig. 8) at the binding energy of 288.65 and 288.27 eV, respectively, which belong to the heptazine ring, are already present. The ratio of the C_1 to C_2 peak areas is 1.02 (close to 1, as expected by the assignments, since the number of carbon C_1 and C_2 should be the same in the heptazine ring). At 550 °C the C–C peak grew while the C–N decreased, but, after the 700 °C treatment, both C–C, C═N and C–N belonging to intermediates as well as to not well-formed products have almost disappeared. It is remarkable to mention that, in all the treatment cases, it is possible to observe the presence of the broad peak at 293.91 eV due to excited electrons of the π^* orbital of heptazine units (hereinafter indicated as π electrons for brevity).

At 450 °C three main deconvolution peaks can be identified as N_1 (ring nitrogen), N_2 (secondary amine), and N_3 (primary amine) (see Fig. 7) at 398.77 eV, 400.27 eV, and 401.40 eV, respectively [13]. The C–N found in C1s is probably included in N_2, but difficult to distinguish as a separated peak. The broad peak at 404.54 eV is assigned to π electrons of the nitrogen of the heptazine ring. At 550 °C a deconvolution peak attributable to C═N is found, and this may indicate that at this temperature there is a general rearrangement of the polymer, probably with further loss of mass by formation of water. The N_2 peak decreased concurrently with the decrease of the C–N peak in C1s. In the case of the N1s spectrum, at 650 °C the remaining peaks are N_1, N_2 and N_3, with peak area ratios 7.2: 2.2: 0.6, when the theoretical ratios are 7:2:1 according to the assignations in Fig. 7. At 700 °C the situation is stabilized. It may also be noticed that the π peak increased from 450 °C to 700 °C, as it happened for the corresponding π peak of C1s.

The evolution of SATS from 450 °C to 700 °C is quite different. At 450 °C, the C1s spectrum (see Fig. 9) shows the presence of

Table 1
Elemental analysis of the reference (melamine cyanurate) and the sulfuric acid-treated sample (SATS) of melamine cyanurate.

	N (wt%)	C (wt%)	H (wt%)	N (mol)	C (mol)	H (mol)	N/C Ratio
Reference							
700 °C	60,54	35,85	1,50	4,32	2,98	1,48	1,45
650 °C	61,60	35,92	1,49	4,40	2,99	1,48	1,47
550 °C	59,75	34,35	1,95	4,27	2,86	1,94	1,49
450 °C	60,35	33,54	2,22	4,31	2,79	2,20	1,54
SATS							
700 °C	60,93	36,10	1,49	4,35	3,01	1,48	1,45
650 °C	60,98	35,79	1,54	4,35	2,98	1,53	1,46
550 °C	59,95	34,51	1,87	4,28	2,87	1,85	1,49
450 °C	54,46	27,94	2,62	3,89	2,33	2,60	1,67

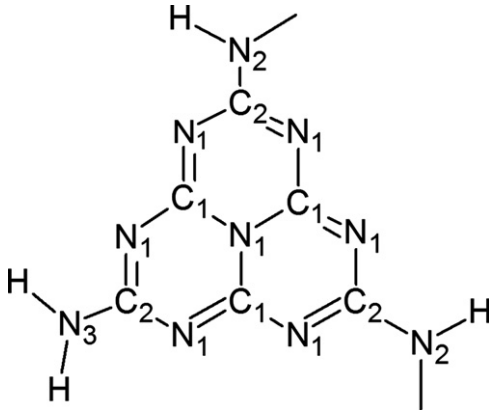

Fig. 7. Repeating unit of the carbon nitride polymer with atom numbering according to their XPS peaks and equivalence.

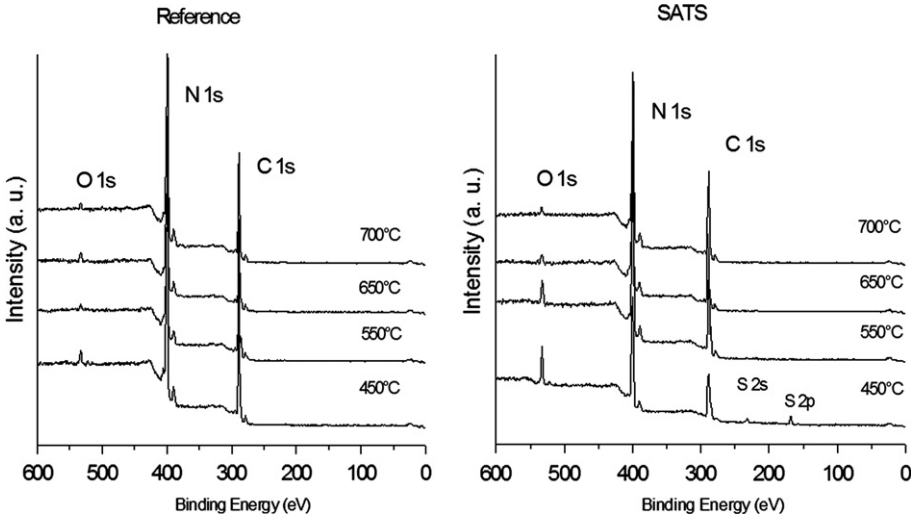

Fig. 6. Full XPS spectra of both the reference and SATS treated in the temperature range 450–700 °C.

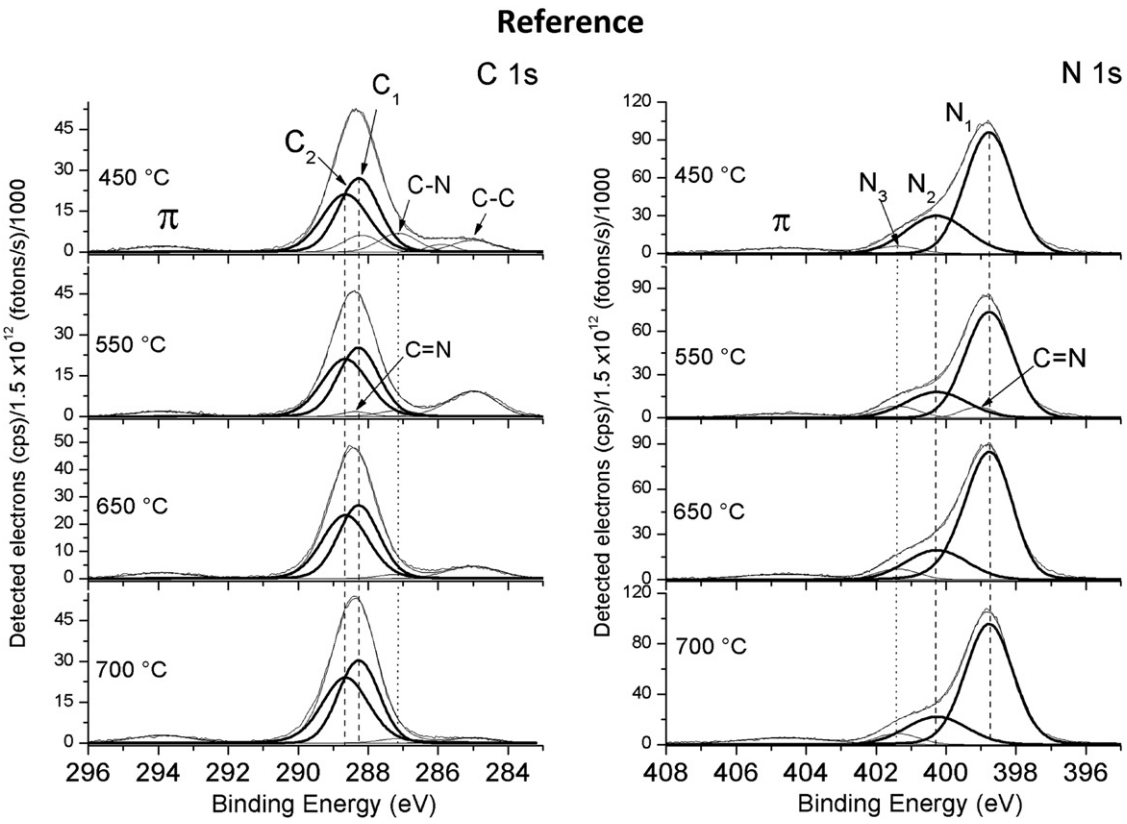

Fig. 8. XPS C1s of the reference treated in the temperature range 450–700 °C.

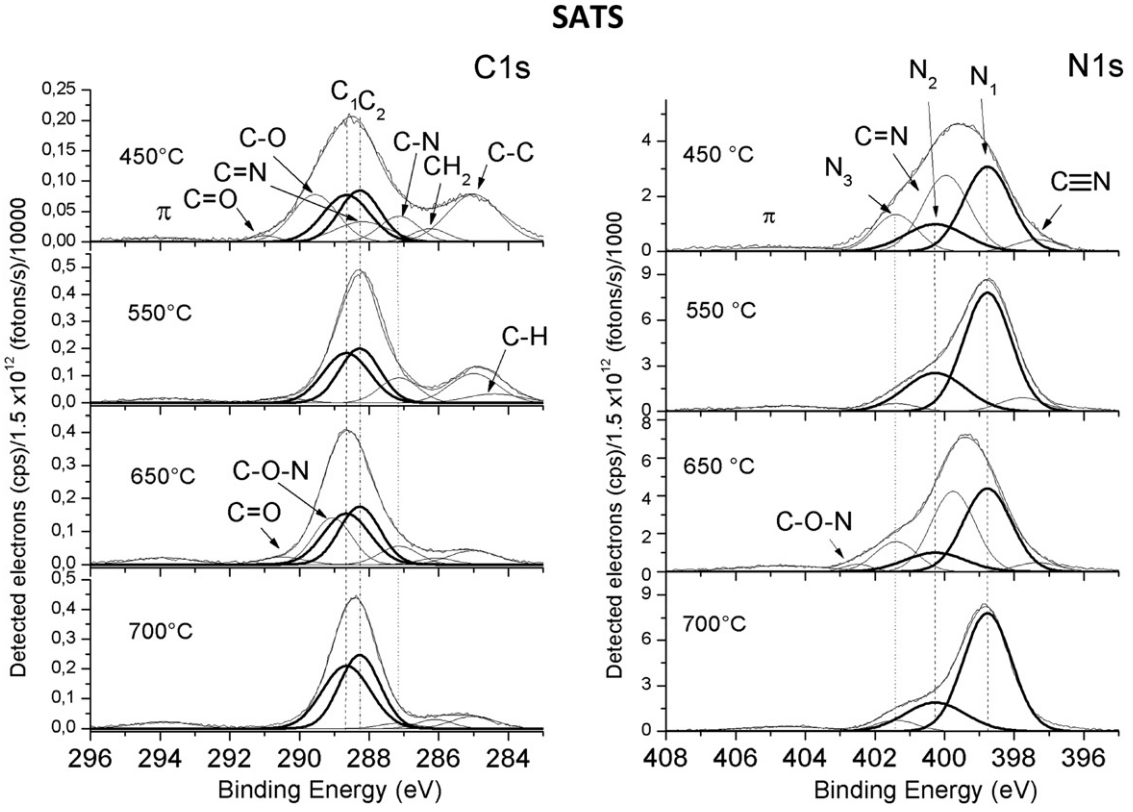

Fig. 9. XPS N1s of the SATS treated in the temperature range 450–700 °C.

bonds between C and O coming probably from cyanuric acid and derived intermediates and byproducts. The prevalence of the peak attributed to C–O at 289.53 eV, instead of that of C═O localized at 291.01 eV, confirms that the mechanism of sulfuric acid catalysis implies the formation of the lactim tautomer (with C–O–H) of cyanuric acid at the expense of the more stable lactam tautomer (with C═O), as found by our group and exposed in a previous report [18]. In addition to C_1 and C_2 that belong to either *s*-triazine or tri-*s*-triazine rings with conjugated double bonds, there are deconvolution peaks between 286 and 285 eV attributed to decomposition products such as hydrocarbons. It is noteworthy to mention that the peak at 287.16 eV is attributed to C–N and the one at 288.18 eV to C═N, which can belong to opened rings and be connected to the found hydrocarbonic carbons, indicating that reaction mechanism towards carbon nitride requires several steps, including rings′ opening and lateral reactions. At 550 °C the peaks attributed to C bound to O almost disappeared, indicating the advancement of dehydration, while C–H appeared at 284.43 eV at expense of the CH_2 peak found at 450 °C. A peak of carbon products was still present at 284.99 eV. At 650 °C carbon bonded to oxygen reappeared with a deconvolution peak at 290.5 eV, while a peak possibly belonging to C–O–N also appeared at 289.07 eV, while the C–N peak at 287.16 eV decreased in comparison with those at lower temperatures. This occurrence can be due to oxygen coming from residual sulfate that decomposed at this temperature, thus indicating that the role of sulfuric acid is more complex than it may seem. At the same time, the carbon peak at 285.00 eV decreased considerably in comparison with the SATS treated at 550 °C.

For SATS treated at 700 °C, it should be noticed that the C_1 and C_2 peaks reached their maximum and that the ratio of C_1 to C_2 is 1.0 as expected (see Fig. 9). It is significant that the broad π peak, related to the heptazine units, increased from 450 °C to 700 °C. Moreover, the C–N peak at 287.16 eV decreased dramatically compared with that of the 650 °C sample. On the other hand, the broad peaks of carbonaceous byproducts between 286 and 285 eV, although much lower than those of the samples treated between 450 °C and 550 °C, seem to be unvaried in comparison with that at 650 °C. Around 650 °C the residual oxygen which came from sulfate oxidized carbon and nitrogen atoms. At 700 °C the product C1s peaks are identical to those of the reference at the same temperature.

The N1s of SATS show a trend parallel to that of C1s and the spectra at the different treatment temperatures (see Fig. 11). N_1, N_2 and N_3 are in the same positions as in the reference. At 450 °C, the peak at 399.93 eV is attributed to C═N, while at 550 °C the N_2 peak, attributed to secondary bridging amines, increased according to crosslinking advancement. The spectrum at 650 °C shows that a rearrangement was occurring in accordance with the C1s peak of the same sample, a peak attributed to C–O–N appeared at 402.55 eV and the peak of C═N reappeared. However, the rearrangement mostly involved carbon with residual oxygen. At 700 °C a situation quite similar to that of the reference was found with N_1, N_2, and N_3 with peak area ratios of 7.2: 2.2: 0.6. It is noteworthy to point out that the π broad peak at 404.68 eV also increased in this case from 450 °C to 700 °C, reaching the same final value than in the reference. These results, together with those of FT-IR and elemental analysis, confirm that the final products obtained at 700 °C for both the reference and SATS are constituted of polymeric carbon nitride.

3.3. Structure and morphology

The XRPD patterns of the reference treated at 450, 500, 550, 650 and 700 °C are reported in Fig. 10. Between 450 °C and 550 °C, it is possible to observe a broad peak at 27.4 ° corresponding to the 002 reflection of an essentially amorphous product with

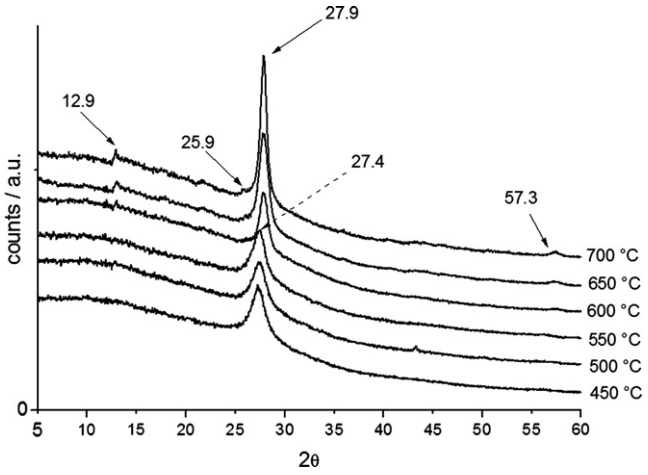

Fig. 10. XRPD patterns of the reference treated in the temperature range 450–700 °C.

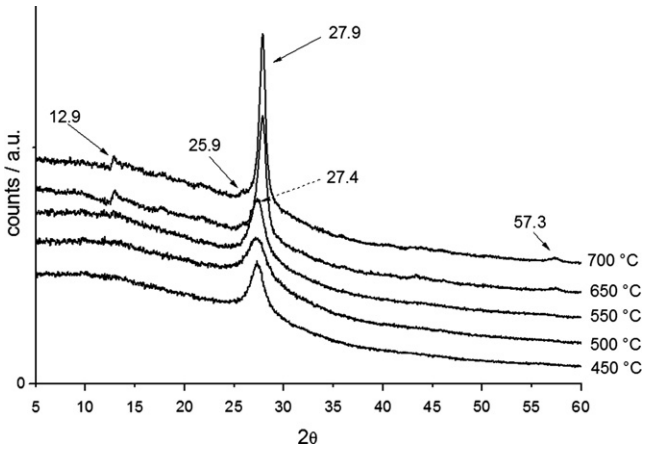

Fig. 11. XRPD patterns for the SATS treated in the temperature range 450–700 °C.

interplanar distance of 3.25 Å. At 650 °C this peak was shifted to 27.9 ° and became sharp and more intense. This peak corresponds to the 002 reflection with an interplanar distance *c*/2 of 3.21 Å, which is a characteristic value of crystalline graphitic carbon nitride. The tightening of the interplanar distance from 3.25 Å to 3.21 Å is probably due to thinning of the polymer sheets, caused by the degradation induced by high temperature treatments (from 450 °C to 700 °C), and the consequent stronger interplanar interaction [22,23]. The other characteristic peak, located at 12.9 ° (interplanar distance of 6.9 Å), was weak and belongs to an in-plane reflection. Other very weak peaks at 18.1 ° and 22.0 ° may belong to intermediates. Another peak at 57.3 ° may correspond to a harmonic of the main 002 reflection [13,20]. Similar patterns with similar trends were found for the SATS treated in the same temperature interval (see Fig. 11). The shifting and sharpening of the 002 reflection are in accordance with both the IR band sharpening with increasing temperature (especially for 700 °C spectra) and the exothermic peak found in thermal analysis around 700 °C attributable to crystallization and tightening.

Fig. 12a and b shows the SEM images of the SATS polymeric carbon nitride for temperatures ranging from 450 °C to 550 °C to be compared with the reference SEM images (Fig. 12c and d). The SATS at 450 °C exhibited particles with a desert rose-like shape with interconnected planar flakes (Fig. 12a), while the reference exhibited more degraded flakes (Fig. 12c). At 550 °C the desert rose-like structure had disappeared (Fig. 12b) and very fragmented

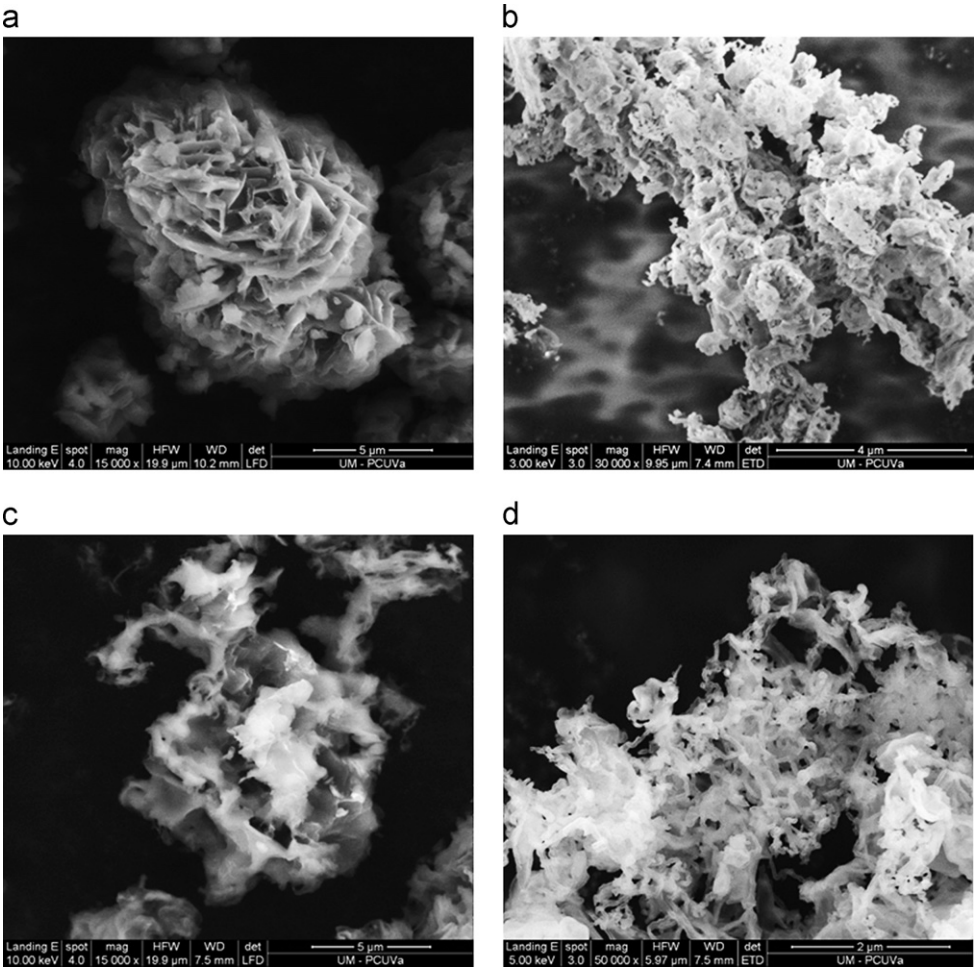

Fig. 12. SEM images. SATS: (a) at 450 °C; (b) at 550 °C. Reference: (c) at 450 °C and (d) at 550 °C.

flakes were present, as for the reference which exhibited even more filamentous, crumpled and tubular particles with a thickness of several nanometers (Fig. 2d). The situation is almost unvaried at 650 °C as it can be seen in the TEM image of SATS (Fig. 13a); however, at 700 °C more corrugated particles appeared (Fig. 13b). The evolution from fragmented particles to globular particles with openings in the walls is even more marked in the reference in the transition from 650 °C to 700 °C (see Fig. 13c and d). Fig. 14a shows an in-plane sheet view, while Fig. 14b shows a sheet edge, an example of the carbon nitride nanosheets (plane stacks are distinguishable) [24], which is around 20 nm thick. An interplanar distance **c**/2 of 3.2 Å, in accordance with XRPD results, was found by analyzing the TEM image of Fig. 14b (notice that graphite *c*/2 is around 3.35 Å [5]). The nanosheets of polymeric carbon nitrides tend to form "entangled", crumpled surfaces, similar in some cases to globes with holes. These conformations seem to be originated from the curled surfaces that tended to enroll and then shrink by effect of the stabilization needed by the particle sheets, which were constituted by several layers (reaching a thickness around 10–40 nm) but not enough to minimize energies to flat surfaces. Thus we conclude that the product for both SATS and the reference was polymeric carbon nitride and both final products (reference and SATS) at 700 °C have similar morphologies, although the intermediates at lower temperatures exhibited significant differences. That is, sulfuric acid favored the reaction increasing the yield without altering the chemical nature of the final product. In summary, the reaction mechanism that incremented yield by means of sulfuric acid can be outlined as follows: sulfuric acid caused the disruption of the melamine cyanurate adduct by stabilizing the lactim tautomer of cyanuric acid [18] and forming melaminium sulfate [14], which decomposed around 400–450 °C releasing H_2SO_4. The slow decomposition of melaminium sulfate is concurrent to the reactions of both heptazine ring formation and polycondensation. In spite of this fact, polycondensation continued to go forward considerably at higher temperatures, as it has been particularly evidenced by XPS. In the absence of a catalyst, the quick sublimation of melamine cyanurate at 430 °C prevented the formation of considerable amounts of polymeric carbon nitride, which occurs around 450 °C.

3.4. Electronic and optical gap characteristics from UV–vis and XPS studies

XPS at low binding energies (0–20 eV) provides useful information on the valence band electrons with respect to the Fermi level E_F, which is taken as a reference of the binding energy of the XPS spectrum. These valence band XPS spectra are shown in Fig. 15 for both reference and SATS. The valence band maximum energy E_V was taken as the energy value at the intersection of the energy axis with the straight line of the linear part of the valence band onset, obtained by the least square method. The difference between this value and the Fermi energy, which is the reference value, gives the position of the Fermi energy with respect to E_V, as indicated in the following equation:

$$\Delta E_F = 0 - E_V = -E_V \quad (1)$$

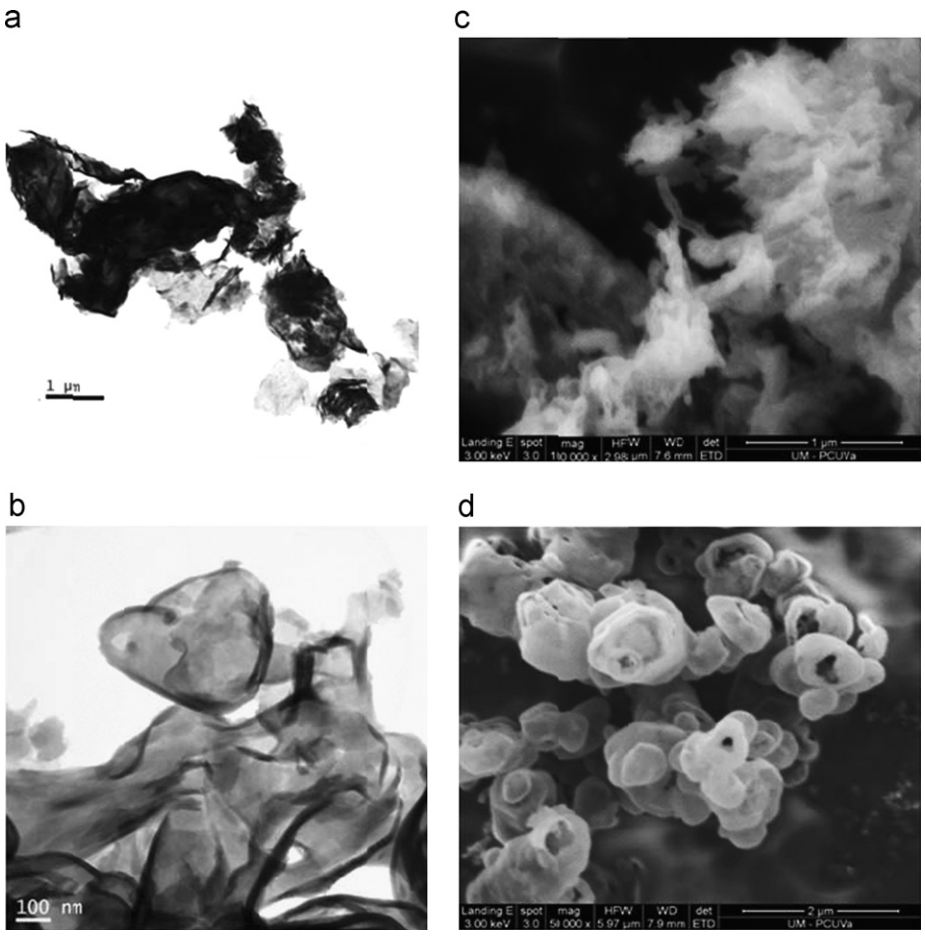

Fig. 13. TEM images. SATS: (a) at 650 °C; (b) at 700 °C. SEM images. Reference: (c) at 650 °C and (d) at 700 °C.

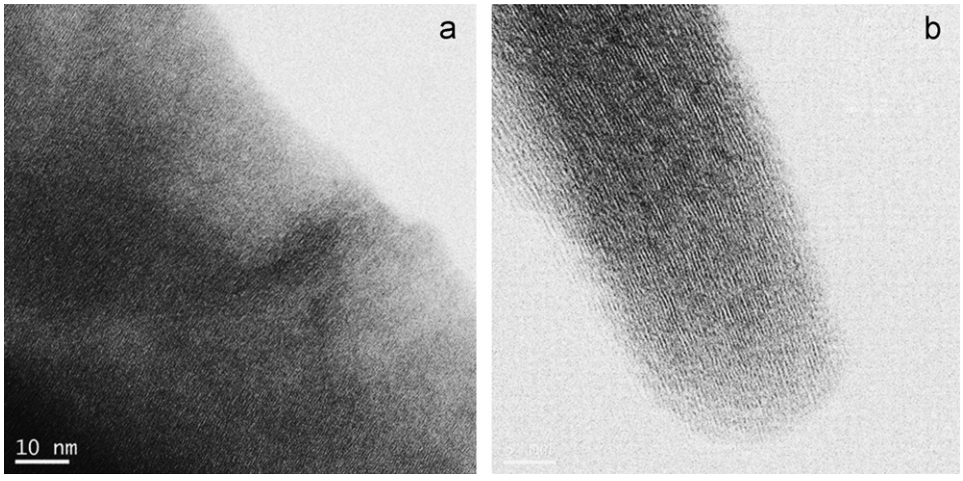

Fig. 14. TEM images. SATS at 650 °C: (a) in-plane flake view and (b) flake edge view.

The UV–vis spectra for both reference and SATS are shown in Fig. 16. It is significant that, apart from the large band around 400 nm, in both cases (reference and SATS) a broad absorption around 470 nm appeared from the sample treated at 650 °C and became a prominent shoulder in the samples treated at 700 °C. This is due to electrons whose energy is located between the valence and conduction band. The band gap E_g and ΔE_F for both SATS and reference are shown in Fig. 17 as a function of the treatment temperature. The values of E_g typical of wide-band gap semiconductors remain between 2.942 eV and 2.789 eV for SATS at 550 °C and at 700 °C, respectively [23]. However, the variation of ΔE_F is considerable. For SATS it changed from 1.617 eV at 450 °C to 1.928 eV at 700 °C, while for the reference it increased from 1.577 eV to 2.093 eV. The evolution of the Fermi level from values slightly above $1/2E_g$ to values well above the $1/2E_g$, as the polymerization advanced, indicates that the product became a

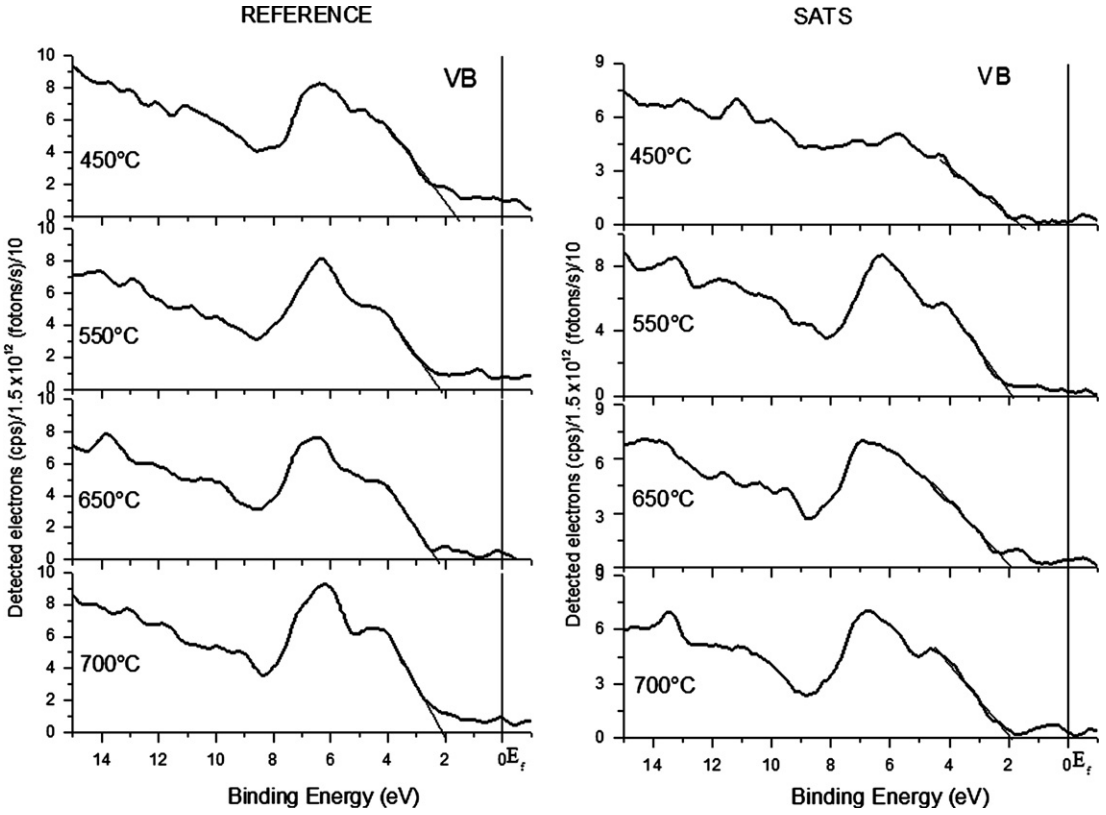

Fig. 15. XPS low binding energy for reference and SATS in the temperature range 450–700 °C. The maximum energy of the valence band E_v is given by the value of the intersection of the straight line extrapolated from the linear region with binding energy axis.

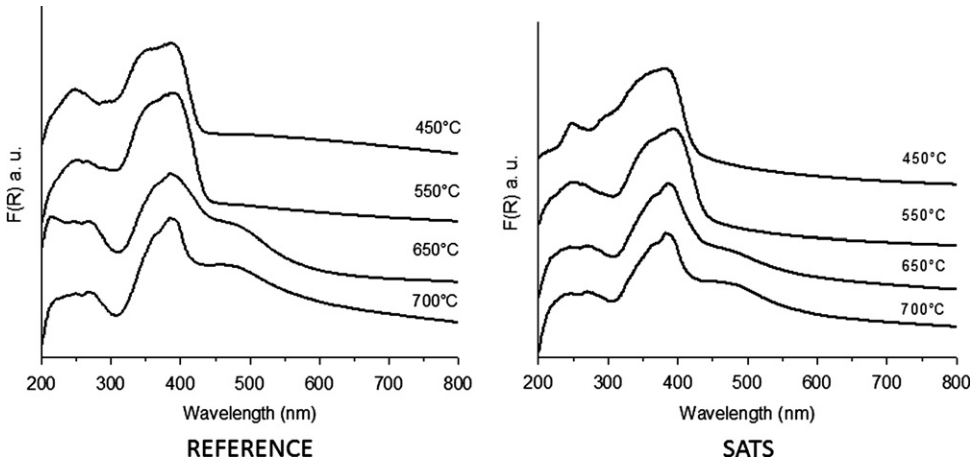

Fig. 16. UV–visible spectra of reference and SATS in the temperature range 450–700 °C.

n-type semiconductor as determined through other means by Zhang et al. [15]. These results obtained combining the XPS data and UV–vis are in agreement with the mentioned shoulder which appeared at around 470 nm in UV–vis spectra. Although the 700 °C samples of both reference and SATS have quite similar E_g and ΔE_F, the evolution of ΔE_F from a minimum at 450 °C to a maximum at 650 °C for the reference, with significant higher values in comparison with SATS, is probably related to the different reaction mechanism caused by the sulfuric acid catalysis. Since the Fermi level coincides with the chemical potential, this indicates that the non-catalyzed route passed through less stable intermediates, explaining the much lower yield.

4. Conclusions

Melamine cyanurate adduct is a suitable reagent and precursor to synthesize polymeric carbon nitride with specific characteristics. The polycondensation reaction is catalyzed by sulfuric acid with a yield around 15%wt at 700 °C in a tapped crucible. The reaction, catalyzed by sulfuric acid, seems to involve not only the Brønsted sites to form the lactim tautomer of cyanuric acid but also the formation of the melaminium sulfate which decomposes at high enough temperatures to allow heptazine ring formation and polycondensation. The products obtained between 650 °C and 700 °C were mainly composed of polymeric carbon nitride nanosheets,

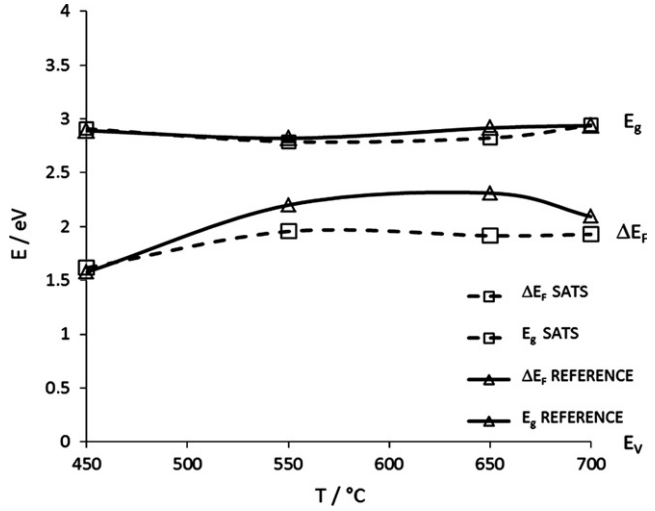

Fig. 17. Optical gap energy E_g, and ΔE_F to respect the maximum valence band energy E_v.

which exhibited curled shapes, in some cases similar to either crumpled globes with openings or tubules. The nitrogen to carbon ratio of the product, obtained with sulfuric acid as a catalyst, was 1.46. The optical gap, typical of a wide band gap semiconductors, is situated around 2.9–2.8 eV, and the Fermi level increased from about 1.6 eV to about 2 eV (from 450 °C to 700 °C), approaching the conduction band, which is indicative of a *n*-type semiconducting behavior for the more developed polymer network (650–700 °C).

Acknowledgments

The authors are grateful to the Universidad de Valladolid for the support to RCD as a visiting professor, and to the Junta of Castilla y León (Spain) for the support to this research through the Proyecto de la Consejería de Educación de la JCyL, No. VA036A12.

References

[1] M.L. Cohen, Phys. Rev. B: Condens. Matter Mater. Phys. 32 (1985) 7988.
[2] A.Y. Liu, M.L. Cohen, Phys. Rev. B: Condens. Matter Mater. Phys. 41 (1990) 10727.
[3] X. Li, J. Zhang, L. Shen, Y. Ma, W. Lei, Q. Cui, G. Zou, Appl. Phys. A: Mater. Sci. Process. 94 (2009) 387.
[4] Y. Zhao, L. Zheng, W. Chu, L. Song, Z. Zhang, D. Yu, Y. Tian, S. Xie, L. Sun, Adv. Mater. 9999 (2008) 1.
[5] R.C. Dante, J. Martin Gil, L. Pallavidino, F. Geobaldo, J. Macromol. Sci. B 49 (2010) 371.
[6] A. Vinu, K. Ariga, T. Mori, T. Nakanishi, S. Hishita, D. Goldberg, Y. Bando, Adv. Mater. 17 (2005) 1648.
[7] H.Z. Zhao, M. Lei, X. Yang, J.K. Jian, X.L. Chen, J. Am. Chem. Soc. 127 (2005) 15722.
[8] J.L. Zimmerman, R. Williams, V.N. Khabashesku, J.L. Margrave, Nano Lett. 1 (2001) 731.
[9] C.B. Cao, F.L. Huang, C.T. Cao, J. Li, H.S. Zhu, Chem. Mater. 16 (2004) 5213.
[10] A. Thomas, A. Fischer, M. Antonietti, J. Müller, R. Schlögl, J.M. Carlsson, J. Mater. Chem. 18 (2008) 4893.
[11] C. Li, X. Yang, B. Yang, Y. Yan, Y. Qian, Mater. Chem. Phys. 103 (2007) 427.
[12] M. Deifallah, P.F. Mc Millan, F. Corà, J. Phys. Chem. C 112 (2008) 5447.
[13] R.C. Dante, P. Martín-Ramos, A. Correa-Guimaraes, J. Martín-Gil, Mater. Chem. Phys. 130 (2011) 1094.
[14] A. Heine, K. Gloe, T. Doert, K.Z. Gloe, Z. Anorg. Allg. Chem. 634 (2008) 452.
[15] J. Zhang, J. Sun, K. Maeda, K. Domen, L. Ping, M. Antonietti, X. Fu, X. Wang, Energy Environ. Sci. 4 (2011) 675–678.
[16] M. Nowak, B. Kauch, P. Szperlich, Rev. Sci. Instrum. 80 (2009) 046107.
[17] H. Yan, Y. Chen, S. Xu, Int. J. Hydrogen Energy 37 (2012) 125.
[18] R.C. Dante, P Martín-Ramos, L.M. Navas-Gracia, F.M. Sánchez-Arévalo, J. Martín-Gil, J. Macromol. Sci. B 52 (2013) 623.
[19] B. Jürgen, E. Irran, J. Senker, P. Kroll, H. Müller, W. Schnick, J. Am. Chem. Soc. 125 (2003) 10288.
[20] D. Foy, G. Demazeau, P. Florian, D. Massiot, C. Labrugère, G. Goglio, J. Solid State Chem. 182 (2009) 165.
[21] E. Horvath-Bordon, E. Kroke, I. Svoboda, H. Fueß, R. Riedel, S. Neeraj, A.K. Cheetham, Dalton Trans. 22 (2004) 3900.
[22] P. Niu, L. Zhang, G. Liu, H. Cheng, Adv. Funct. Mater. 22 (2012) 4763.
[23] G. Zhang, J. Zhang, M. Zhang, X. Wang, J. Mater. Chem. 22 (2012) 8083.
[24] S. Yang, X. Feng, X. Wang, K. Müllen, Angew. Chem. Int. Ed. 50 (2011) 5339.